Tunable narrow-bandpass filter based on an asymmetric photonic bandgap structure with a dual-mode liquid crystal

Hsiao-Tsung Wang,[1] Ivan V. Timofeev,[2,3] Kai Chang,[1] Victor Ya. Zyryanov,[2] and Wei Lee[1,*]

[1]*College of Photonics, National Chiao Tung University, Guiren Dist., Tainan 71150, Taiwan*
[2]*Kirensky Institute of Physics, Krasnoyarsk Scientific Center, Siberian Branch of Russian Academy of Sciences, Krasnoyarsk 660036, Russia*
[3]*Siberian Federal University, Krasnoyarsk 660041, Russia*
**wlee@nctu.edu.tw*

Abstract: A one-dimensional asymmetric photonic crystal with dual-frequency liquid crystal as a central defect layer was demonstrated. Such asymmetric structure was characterized by the dramatic increase in intensity of the electric field of light localized at the overlapped photonic bandgap edges, thereby enhancing the observed transmittance of the spectral windows originating from the defect layer. The defect layer was made of a dual-mode liquid crystal that exhibited not only electrical tunability and switchability but also optical bistability. Consequently, tunable and bistable defect modes can be realized in the photonic structure. This asymmetric photonic crystal structure is promising and should be further explored for photonic device applications.

OCIS codes: (230.3720) Liquid-crystal devices; (230.5298) Photonic crystals.

References and links

1. E. Yablonovitch, "Inhibited spontaneous emission in solid-state physics and electronics," Phys. Rev. Lett. **58**(20), 2059–2062 (1987).
2. S. John, "Strong localization of photons in certain disordered dielectric superlattices," Phys. Rev. Lett. **58**(23), 2486–2489 (1987).
3. O. Painter, R. K. Lee, A. Scherer, A. Yariv, J. D. O'Brien, P. D. Dapkus, and I. Kim, "Two-dimensional photonic band-gap defect mode laser," Science **284**(5421), 1819–1821 (1999).
4. H. Coles and S. Morris, "Liquid-crystal lasers," Nat. Photonics **4**(10), 676–685 (2010).
5. C.-Y. Chen, C.-L. Pan, C.-F. Hsieh, Y.-F. Lin, and R. P. Pen, "Liquid-crystal-based terahertz tunable Lyot filter," Appl. Phys. Lett. **88**(10), 101107 (2006).
6. P. Bermel, C. Luo, L. Zeng, L. C. Kimerling, and J. D. Joannopoulos, "Improving thin-film crystalline silicon solar cell efficiencies with photonic crystals," Opt. Express **15**(25), 16986–17000 (2007).
7. Y.-K. Ha, Y.-C. Yang, J.-E. Kim, H.-Y. Park, C.-S. Kee, H. Lim, and J.-C. Lee, "Tunable omnidirectional reflection bands and defect modes of a one-dimensional photonic band gap structure with liquid crystals," Appl. Phys. Lett. **79**(1), 15–17 (2001).
8. G. E. Nevskaya, S. P. Palto, and M. G. Tomilin, "Liquid-crystal-based microlasers," J. Opt. Technol. **77**(8), 473–486 (2010).
9. Y.-T. Lin, W.-Y. Chang, C.-Y. Wu, V. Y. Zyryanov, and W. Lee, "Optical properties of one-dimensional photonic crystal with a twisted-nematic defect layer," Opt. Express **18**(26), 26959–26964 (2010).
10. A. Baldycheva, V. A. Tolmachev, K. Berwick, and T. S. Perova, "Multi-channel Si-liquid crystal filter with fine tuning capability of individual channels for compensation of fabrication tolerances," Nanoscale Res. Lett. **7**(7), 387 (2012).
11. D. C. Zografopoulos, E. E. Kriezis, B. Bellini, and R. Beccherelli, "Tunable one-dimensional photonic crystal slabs based on preferential etching of silicon-on-insulator," Opt. Express **15**(4), 1832–1844 (2007).
12. G. Calo and L. Mescia, "Tunability of photonic band gap notch filters," IEEE Trans. NanoTechnol. **7**(3), 273–284 (2008).
13. A. C. Tasolamprou, B. Bellini, D. C. Zografopoulos, E. E. Kriezis, and R. Beccherelli, "Tunable optical properties of silicon-oninsulator photonic crystal slab structure," J. Eur. Opt. Soc. – Rapid **4**, 09017 (2009).

#208485 - $15.00 USD Received 21 Mar 2014; revised 7 Jun 2014; accepted 8 Jun 2014; published 12 Jun 2014

14. R. Ozaki, T. Matsui, M. Ozaki, and K. Yoshino, "Electrically color-tunable defect mode lasing in one-dimensional photonic-band-gap system containing liquid crystal," Appl. Phys. Lett. **82**(21), 3593–3595 (2003).
15. J. Yoon, W. Lee, J. M. Caruge, M. Bawendi, E. L. Thomas, S. Kooi, and P. N. Prasad, "Defect-mode mirrorless lasing in dye-doped organic/inorganic hybrid one-dimensional photonic crystal," Appl. Phys. Lett. **88**(9), 091102 (2006).
16. I.-A. Yao, C.-L. Yang, C.-J. Chen, J.-P. Pang, S.-F. Liao, J.-H. Li, and J.-J. Wu, "Bistability of splay and π twist states in a chiral-doped dual frequency liquid crystal cell," Appl. Phys. Lett. **94**(7), 071104 (2009).
17. C.-Y. Wu, Y.-H. Zou, I. V. Timofeev, Y.-T. Lin, V. Y. Zyryanov, J.-S. Hsu, and W. Lee, "Tunable bi-functional photonic device based on one-dimensional photonic crystal infiltrated with a bistable liquid-crystal layer," Opt. Express **19**(8), 7349–7355 (2011).
18. T. J. Scheffer and J. Nehring, "Accurate determination of liquid-crystal tilt bias angles," J. Appl. Phys. **48**(5), 1783–1792 (1977).
19. F.-C. Lin and W. Lee, "Color-reflective dual-frequency cholesteric liquid crystal displays and their drive schemes," Appl. Phys. Express **4**(11), 112201 (2011).
20. P. Bos and K. Koehler-Beran, "The pi-cell: a fast liquid-crystal optical-switching device," Mol. Cryst. Liq. Cryst. (Phila. Pa.) **113**(1), 329–339 (1984).
21. S.-H. Chen and C.-L. Yang, "Dynamics of twisted nematic liquid crystal pi-cells," Appl. Phys. Lett. **80**(20), 3721–3723 (2002).
22. I. V. Timofeev, Y.-T. Lin, V. A. Gunyakov, S. A. Myslivets, V. G. Arkhipkin, S. Y. Vetrov, W. Lee, and V. Y. Zyryanov, "Voltage-induced defect mode coupling in a one-dimensional photonic crystal with a twisted-nematic defect layer," Phys. Rev. E Stat. Nonlin. Soft Matter Phys. **85**(1), 011705 (2012).
23. H.-T. Wang, J.-D. Lin, C.-R. Lee, and W. Lee, "Ultralow-threshold single-mode lasing based on a one-dimensional asymmetric photonic bandgap structure with liquid crystal as a defect layer," Opt. Lett. **39**(12), 3516–3519 (2014).

1. Introduction

Over the past two decades photonic crystals (PCs) with their structural periods comparable to optical wavelengths have been studied extensively [1,2]. The propagation of electromagnetic waves through a PC is forbidden over a spectral region that defines a photonic band gap (PBG) for the periodic structure. With the simplest framework, a one-dimensional (1-D) PC can be constructed by multilayer dielectric materials, allowing the structure to be fabricated and simulated with relative ease. The introduction of a defect layer into a PC breaks its characteristic periodicity, generating defect modes in the PBG. The defect modes have different applications, such as optical cavity lasers [3,4], spectral filters [5], and light-trapping solar cells [6]. Consequently, photonic structures possessing tunable defect modes have attracted a lot of attention recently. Owing to its optical anisotropy and susceptibility to external stimuli, many theoretical [7,8] and experimental [9,10] studies employing liquid crystal (LC) as defect layers to achieve tunability of defect modes or photonic bandgap structures [11–13] have been reported. The wavelength-tunable defect-mode lasing in a multilayer PC infiltrated with a central nematic layer is, indeed, a momentous step for PC/LC hybrid systems [14]. Unfortunately, great discrepancies often existed between experimental data and overestimated simulations [15]. While these previous studies concentrated on wavelength tunability of defect modes in hybrid PBG structures, no obvious effort has been made to promote transmittance of defect modes especially in undyed systems beyond laser applications. In this work we investigated, by simulations and experiments, the spectral properties of an asymmetric PC structure constructed by heterojunction of two distinct multilayer substrates sandwiching a LC layer. The resulting defect modes showed high transmittance near the boundary between the two individual PBGs due to their overlapped band edges. The dual-frequency (DF) bistable chiral- splay nematic (BCSN) layer possessed two stable states—the splay state and π-twist state—and a voltage-sustained bend state [16]. In the bistable (or memory) mode, the defect modes existed with complementary nature at null voltage in the two stable states; in the voltage-sustained (or dynamic) mode, the defect modes had a wider tunable range than that of PC hybrid cells containing another bistable LC [17]. Therefore, the dual-mode PC/DF-BCSN devices were characterized by their defect modes with optical memories and electrical tunability. To the best of our knowledge these are the first 1-D asymmetric PC/LC structures fabricated in a laboratory.

#208485 - $15.00 USD Received 21 Mar 2014; revised 7 Jun 2014; accepted 8 Jun 2014; published 12 Jun 2014

2. Experimental

Figure 1 depicts the structure of a specific 1-D PC/DF-BCSN confined between two dielectric mirrors with the integer $N = 4$. Each multilayer was generally composed of a $(2N + 1)$-layer stack of alternating high-refractive-index material Ta_2O_5 ($n_H = 2.18$) and low-refractive-index material SiO_2 ($n_L = 1.47$) deposited on an indium–tin-oxide (ITO) glass substrate. The multilayers (i.e., PC 1 and PC 2) were specially designed to yield overlapped PBGs near the band edges with dissimilar central reflection wavelengths. The simulation results by means of the 4 × 4 Berreman matrix are shown in Fig. 2 for a sandwiched parallel-alignment LC as the central defect layer. Instead of using a fully vectorial numerical model, all of the simulations of the LC director profile in this study were reasonably carried out with use of 1-D model for the 1-D PC structure. Here the cell geometry and materials parameters were adopted for simulation: the extraordinary refractive index $n_e = 1.718$ and the ordinary refractive index $n_o = 1.496$ for the LC, the thickness of defect layer $d = 2\ \mu$m, and the optical thicknesses $4n_Hd_{H1} = 4n_Ld_{L1} = 450$ nm and $4n_Hd_{H2} = 4n_Ld_{L2} = 600$ nm in the first and second PCs, respectively. Figure 2 reveals a high-transmittance defect mode in the overlapped PBG-edge region. However, a few low-transmittance peaks also appear in the PBGs, which can be suppressed with increasing N. The full width at half maximum (FWHM) of the distinguished defect-mode peak at ~530 nm becomes narrower and the PBG edges steeper as the number N grows larger. The simulated data provided a reasonable guide for real cell design.

To achieve a broader tunable range and consider a larger tolerance for cell fabrication to ensure the overlap of the stop bands, we chose $N = 4$ and adjusted the optical thickness of each dielectric layer to produce two PC substrates with their band gaps centered at 460 and 600 nm. The polyimide SE-8793 (Nissan Chemical) was spin-coated on the top of each dielectric multilayer, and the formed alignment layers were rubbed unidirectionally. The pretilt angle was approximately 4° in the two stable states as measured using the conventional crystal-rotation method [18]. Each assembled cell has a gap as the thickness of the LC defect layer close to 2 μm (simulation condition); the gap was determined by solidified UV gel by exposure to the UV light.

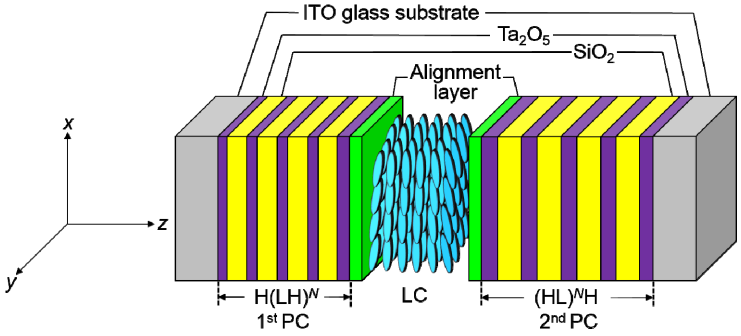

Fig. 1. Schematic of a 1-D asymmetric PC containing DF-BCSN as the central defect layer. The single layer thicknesses of the high- and low-refractive-index dielectric coatings in the first (second) multilayered substrate are d_{H1} (d_{H2}) and d_{L1} (d_{L2}), respectively.

#208485 - $15.00 USD Received 21 Mar 2014; revised 7 Jun 2014; accepted 8 Jun 2014; published 12 Jun 2014

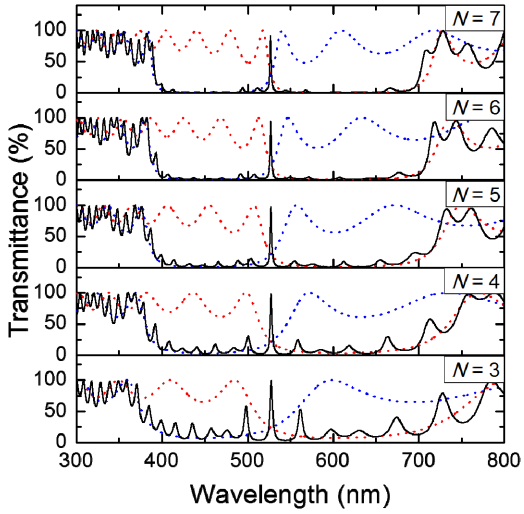

Fig. 2. Simulated transmittance spectra of a 1-D asymmetric multilayer PC comprising nematic LC as the central defect layer with N = 3, 4, 5, 6, and 7 (black solid lines). The blue and red dotted curves are the spectra of the first and second PC substrates showing their central reflection at wavelengths of 450 nm and 600 nm, respectively. Optical extinction is ignored.

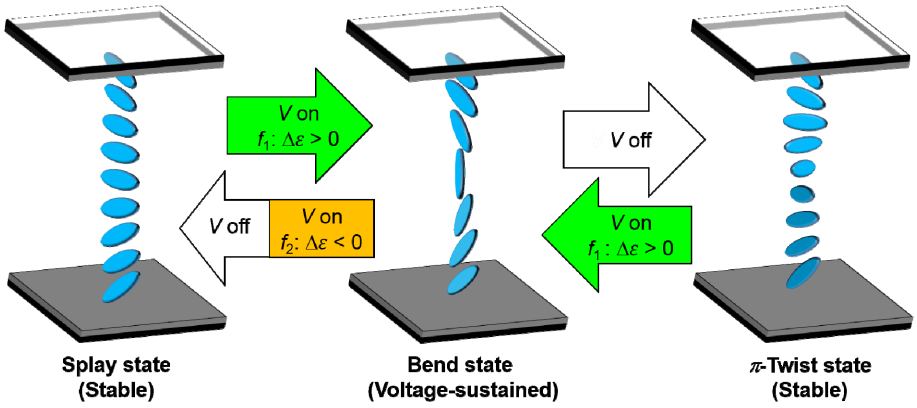

Fig. 3. Switching mechanisms and configurations of a DF-BCSN cell in various states.

The LC used was a mixture of a DF nematic host (HEF-951800-100, HCCH) and a left-handed chiral dopant (HEB, Yung Zip Chemical) [19]. The nematic host possessed dielectric anisotropy $\Delta\varepsilon$ = + 2.6 at 1 kHz and –3.2 at 100 kHz, with crossover frequency $f_c \approx$14 kHz and birefringence Δn = 0.222. The chiral agent blended with DFLC resulted in a thickness-to-pitch ratio d/p ~–0.25 in cells, which yielded equal free energy in the splay and π-twist states. The laboratory spectra of the PC/DF-BCSN cells were acquired with a spectrophotometer (Ocean Optics HR-2000 +). An arbitrary function generator (Tektronix AFG-3021B) was used to supply square-wave voltage to switch the PC/DF-BCSN cells between the bistable mode and voltage-sustained mode.

3. Results and discussion

Figure 3 illustrates the operation principle of a DF-BCSN or PC/DF-BCSN cell. When a field is applied at a low driving frequency f_1, the initial stable splay state is switched to the voltage-sustained bend state. The tunability of defect modes in a PC/DF-BCSN cell is the largest during this transition because the refractive index of the BCSN can be modulated virtually from n_e to n_o as a result of field-induced director reorientation. Once the voltage is removed,

#208485 - $15.00 USD Received 21 Mar 2014; revised 7 Jun 2014; accepted 8 Jun 2014; published 12 Jun 2014

the bend state will relax to the left-helix-twist state by the flow effect in a π-cell [20] in which the corresponding free energy is minimized. If the driving frequency is switched from f_1 to a high frequency f_2 instantly in the high-tilt bend state, the LC molecules will return to the splay state via the backflow effect in conjunction with the revertible dielectric characteristic of a typical DF-LC. The switching time is in a few milliseconds in the transition from the splay or twist state to the bend state at a low-frequency driving voltage. However, the nucleation takes place inevitably during the bend-to-splay state transition (induced by a high-frequency voltage) due to the discontinuous transition of the LC molecules. This leads to the tip-over phenomenon [21] of the middle-layer LC in the transition process and, in turn, results in a prolonged response with a switching time of several seconds (1–3 s).

The simulated and experimental spectra of a PC/DF-BCSN cell (for $N = 4$) in two stable states are shown in Fig. 4. Compared with the simulation data, the transmittance of the defect modes was not as high in the experimental spectra, which was attributable to experimental uncertainties such as in thicknesses of the dielectric thin films and the LC layer as well as to light scattering caused by the structural interface roughness. In the splay state, the measured transmittance of the distinctive defect-mode peak marked 75% at ~535 nm and its FWHM was *ca*. 8 nm. Since the different configurations of LC molecules led to distinct light confinement conditions for the two stable states, two sets of defect modes were obtained at 0 V. Note that the spectral profile of the defect modes looks "fragmentary" in the π-twist state in that both O- and E-mode components coexist (i.e., cases where the light polarization is perpendicular and parallel to the LC director, respectively) in the spectrum [9,22].

Here we further investigated the spatial distribution of the local intensity inside the PC/DF-BCSN LC cell. The strong oscillations of local intensity for O-mode at 534.6 nm in the splay state is observed in Fig. 5, which manifests the large energy confined in the central defect layer by means of the asymmetric PC structure. On the other hand, Fig. 5 also indicates that the spatial distribution of the local intensity is damped in the π-twist state on account of the dissipation of electromagnetic waves in the π-structured LC layer.

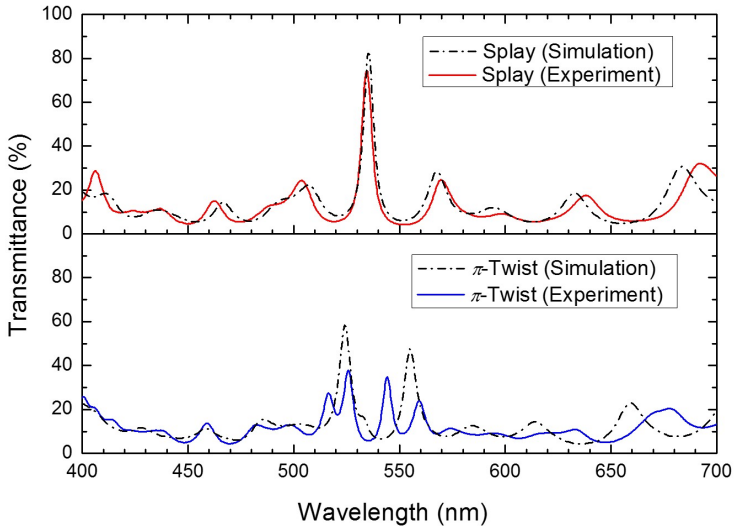

Fig. 4. Simulated (dash-dotted lines) and laboratory (solid lines) spectra of the asymmetric PC/DF-BCSN cell ($N = 4$) in two stable states without any polarizers. Note that the multilayer thicknesses have been acceptably tuned to match the experimental results: d_{SiO2_PC1} = 76.0 nm, d_{SiO2_PC2} = 105.8 nm, d_{Ta2O5_PC1} = 51.5 nm and d_{Ta2O5_PC2} = 71.5 nm in accordance with the mirror spectra. The simulations were sophisticatedly performed with the director profile within the LC defect layer divided into 100 sublayers, taking the optical extinction and dispersion into account.

#208485 - $15.00 USD Received 21 Mar 2014; revised 7 Jun 2014; accepted 8 Jun 2014; published 12 Jun 2014

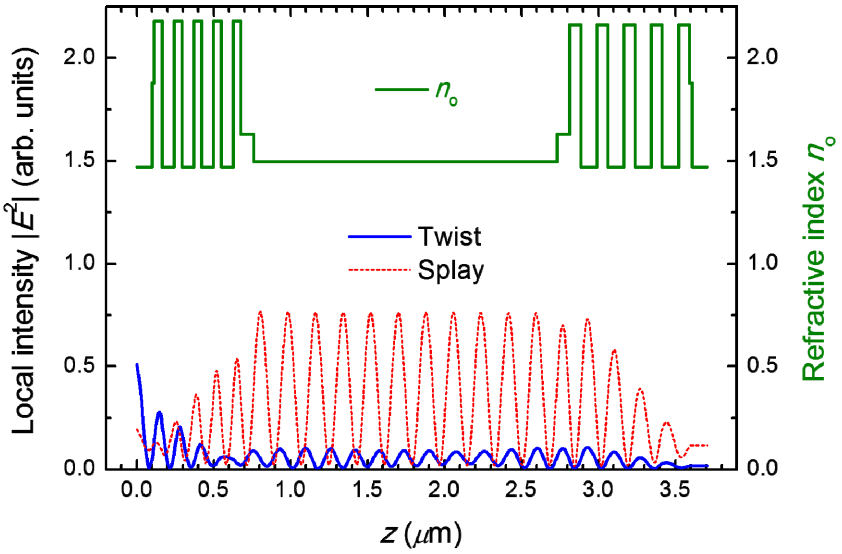

Fig. 5. Spatial distributions of the refractive index n_o (green curve) and local field intensity $|E|^2$ inside the PC/DF-BCSN cell in the splay state (red curve) as well as the π-twist state (blue curve) for O-mode at λ = 535.8 nm. Parameters are the same as used in Fig. 4.

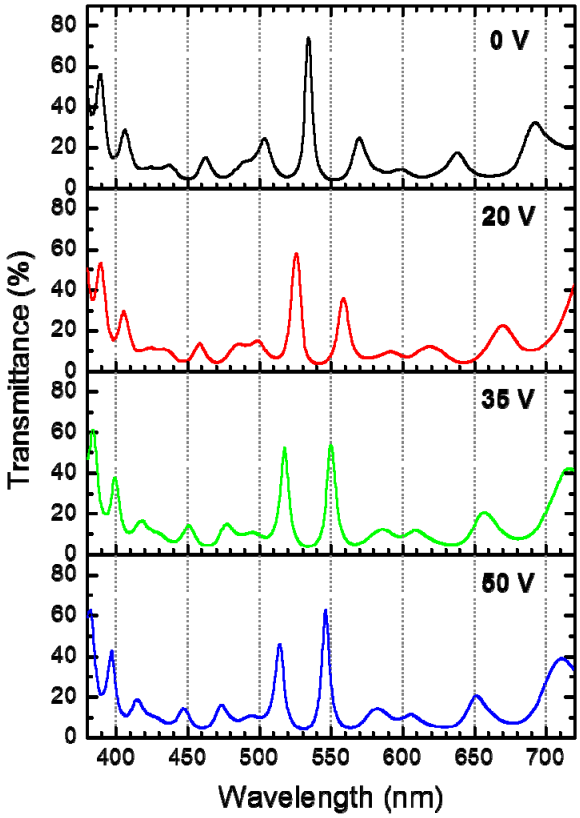

Fig. 6. Experimental transmittance spectra of the tunable defect modes from the splay state to the bend state induced by an applied voltage at a low frequency of 1 kHz.

#208485 - $15.00 USD Received 21 Mar 2014; revised 7 Jun 2014; accepted 8 Jun 2014; published 12 Jun 2014

Figure 6 shows the defect-mode tunability characteristics in a series from the stable splay state (0 V) to the voltage-sustained bend state at 50 V of the PC/DF-BCSN cell. The effective refractive index (n_{eff}) of the LC changes with the molecular tilt angle so that the defect modes can be modulated by changing the ac applied voltage. As the defect modes shift in wavelength with increasing voltage, the transmittance is suppressed in the non-overlapped regions in the two PBGs. Therefore, one can clearly see the rise in transmittance of one defect-mode peak accompanied by the transmittance drop of the other defect-mode peak. The defect-mode transmittance reaches the maximum at the intersection of the two PBGs where the FWHM becomes narrower. In accordance with Fig. 6, the defect mode shifted about 23 nm from 0 V to 50 V and the two defect-mode peaks became equally high at ~35 V. The tunable range can be extended by increasing the overlapped region of the two PBGs.

4. Conclusions

In summary, we have demonstrated a new asymmetric structure of 1-D multilayer PC with DF-BCSN LC as a central defect layer. Experimental and simulated transmittance spectra attested the idea and manifested the feasibility of this design. Compared with a typical symmetric PC counterpart, the asymmetric structure gives rise to remarkable increase in transmittance of defect-mode peaks and exhibits a much wider range of the resulting PBG. By switching between two stable states, the PC/DF-BCSN cell exhibits complementary sets of defect modes and high-contrast defect-mode transmittance in the overlapped region of the two PBGs. Furthermore, the defect modes in the voltage-sustained bend state are electrically tunable, shifting to shorter wavelengths with increasing voltage. The asymmetric 1-D multilayer PC structure greatly enhances the localized field intensity, which leads to a prolonged dwell time of photons at the band edges. As such, the asymmetric 1-D PC/LC structure can be applied to ultralow-threshold lasers [23]. Besides, the dual-mode switching properties of the PC/DF-BCSN cells have potential in energy-efficient optical switches, integrated photonic devices, and multichannel light filters. Moreover, applications in tunable optical communications are also possible because the central reflection wavelengths of the dielectric mirrors can be easily changed to fall into the near-infrared region while remaining the switching properties of a PC/DF-BCSN cell in the single mode (splay state), multimode (voltage-sustained state), and extinction mode (twist state).

Acknowledgments

This work was supported by the Ministry of Science and Technology of Taiwan through Grant No. NSC 101-2112-M-009-018-MY3 as well as Grant No. NSC 103-2923-M-009-003-MY3 dedicated to a joint project between Taiwan and Russia. Both I. V. Timofeev and V. Ya. Zyryanov would like to thank the Russian Foundation for Basic Research (project No. 14-02-3124814) and the Siberian Branch of the Russian Academy of Sciences (grants Nos. 43, 24.29 and 101).